VALIDATION OF ATMOSPHERIC BOUNDARY LAYER TURBULENCE MODEL BY ON-SITE MEASUREMENTS

by

Žarko M. STEVANOVIĆ *, Nikola S. MIRKOV, Žana Ž. STEVANOVIĆ, and Andrijana D. STOJANOVIĆ

Laboratory for Thermal Engineering and Energy, Vinča Institute of Nuclear Sciences, Belgrade, Serbia

Original scientific paper
UDC: 551.511/.513:517.957:532.517.4
DOI: 10.2298/TSCI1001199S

Modeling atmosperic boundary layer with standard linear models does not sufficiently reproduce wind conditions in complex terrain, especially on leeward sides of terrain slopes. More complex models, based on Reynolds averaged Navier-Stokes equations and two-equation k-ε turbulence models for neutral conditions in atmospheric boundary layer, written in general curvilinear non-orthogonal co-ordinate system, have been evaluated. In order to quantify the differences and level of accuracy of different turbulence models, investigation has been performed using standard k-ε model without additional production terms and k-ε turbulence models with modified set of model coefficients. The sets of full conservation equations are numerically solved by computational fluid dynamics technique. Numerical calculations of turbulence models are compared to the reference experimental data of Askervein hill measurements.

Keywords: *atmospheric boundary layer, turbulence modelling, neutral atmosphere*

Introduction

In recent years modelling of micro and meso scales of atmospheric boundary layer phenomena has received growing interest. One of the reasons for such situation is the need for better wind field predictions which are connected, along with local climatology and orography, with the procedures of selection of wind farm sites, also known as siting.

One of the basic phenomena associated to air motion is its turbulence nature; for that reason there have been many attempts to make turbulence models as accurate as acceptable. For the sake of simplicity, most models make use of a simple gradient transfer hypothesis where only a turbulent exchange coefficient has to be defined. At the beginning, this coefficient is often evaluated by a mixing-length hypothesis, where the mixing length is taken as height dependent. However, for air flows over highly irregular terrain; it is not always obvious how to apply a mixing-length with respect to a varying underlying ground surface. The complexity arises when

* Corresponding author; e-mail: zare@vinca.rs

atmosphere conditions are different than neutral one, when the temperature becomes an active scalar, producing additional force of air motion.

Actually, a few models have tried to circumvent this problem by use of second-order closure model [1]. This is a rather time consuming approach due to many additional equations needed for second order turbulence modelling and is not practicable for most atmospheric boundary layer modelers at present. Two-equation turbulence models, based on the linear eddy-viscosity concept, have been used as a compromise. The most popular and frequently used two-equation turbulence model is well known k-ε model.

However, the popularity of the k-ε turbulence model in engineering applications raises the question of whether it could be used for micro and meso scales modelling in the atmospheric boundary layer. Applying the standard k-ε turbulence model, used in engineering applications to atmospheric flows, yields unrealistic results. Mostly, it is unable to reproduce the right level of turbulence in the weak shear layer away from the ground, where the turbulent viscosity is over predicted [2]. Some modifications of standard k-ε turbulence model have been proposed, almost modifying the set of model's coefficients based on experimental evidence of open terrain [3]. This paper deals with accuracy investigation of different k-ε turbulence model modification, known as: standard model (STKE), boundary layer modification (BLKE), Chen-Kim (CKKE), and renormalization-group (RNG) modification of k-ε turbulence model. All of these simulations are compared to the full-scale experiment performed at Askervein hill (Scotland) [4, 5].

Mathematical model of wind resources

There is renewed interest in recent times in considering equations of mathematical physics written in general curvilinear coordinates with dependent variables as physical components of tensors. This trend is more apparent in fluid dynamical researches where solutions are sought for arbitrary geometries and thus the need for general geometries is unavoidable.

A key result is that if λ is a vector and a_i are the base vectors for a co-ordinate system x^i then in the representation of $\lambda = a_i \lambda_i$, where λ_i are the contravariant components, the vectors $a_l \lambda^1$ *etc.* are parallel to the coordinate curves. Thus, one can interpret λ as the diagonal of a parallelepiped. If λ is a small vector then the magnitudes of the edge vectors are $(g_{11})^{1/2}\lambda^1$, $(g_{22})^{1/2}\lambda^2$, $(g_{33})^{1/2}\lambda^3$. In essence, the length $(g_{ij}\lambda^i\lambda^j)^{1/2}$ equals the length of the diagonal of a parallelepiped whose sides are parallel to the co-ordinate curves and whose edges are of length $(g_{ii})^{1/2}\lambda^i$ (no sum).

The above result lies at the foundation of the definition of physical components of tensors. Thus, the analytical definition of the physical components of a vector u (*e. g.* fluid velocity) is $u_{(i)} = (g_{ii})^{1/2} u_i$ (no sum). Using the standard result $u^i = g^{ik}u_k$ we also have $u_{(i)} = (g_{\mathrm{ii}})^{1/2} g^{ij} u_j$ (sum on j).

Applied mathematical model in this study involves the full set of the differential equations: mass and momentum conservation, coupled with the turbulence k-ε model transport equations with modified set of turbulence model coefficients. Using contravariant physical components of wind velocity vector $U^{(j)}$ in an arbitrary curvilinear co-ordinate frame $x^{(j)}$ above selected terrain, these equations can all be expressed in the following general conservation form:

$$\frac{\Delta}{\Delta x^{(j)}} \quad \rho U^{(j)} \Phi \quad \Gamma_\Phi g^{(jm)} \frac{\partial \Phi}{\partial x^{(m)}} \qquad S_\Phi \tag{1}$$

The terms and coefficients occurring in this expression depend on the conservation equation under consideration, and have to be specified individually (tab. 1). In the case of Carte-

sian co-ordinate system, previous equation has the standard form; however, writing general conservation equation in an arbitrary curvilinear co-ordinate system, used tensor differential operators have to be:

$$\frac{\partial}{\partial x^{(j)}} \quad \frac{1}{\sqrt{g_{ij}}} \frac{\partial}{\partial x^{j}} \tag{2}$$

$$\frac{\Delta}{\Delta x^{(j)}} \quad \sqrt{\frac{g_{ij}}{\left|\det(g_{ij})\right|}} \frac{\partial}{\partial x^{(j)}} \sqrt{\frac{\left|\det(g_{ij})\right|}{g_{ij}}} \tag{3}$$

In the momentum equations, the physical analogue of the standard Christofel's symbol of the second kind is given by:

$$\begin{matrix} i \\ jk \end{matrix} \quad \sqrt{\frac{g_{ij}}{g_{jj} g_{kk}}} \quad \begin{matrix} i \\ jk \end{matrix} \quad \delta_i^j \frac{g_{jm}}{g_{ij}} \quad \begin{matrix} m \\ jk \end{matrix} \tag{4}$$

In the turbulence production term G, the contravariant partial derivation of velocity has the form:

$${}_{(j)}U^{(i)} \quad \frac{\partial U^{(i)}}{\partial x^{(j)}} \quad U^{(m)} \quad \begin{matrix} i \\ mj \end{matrix} \tag{5}$$

The constitutive relation of the Newton's stress hypothesis is used to express the normal and viscous stress tensors:

$$P \quad p \quad \frac{2}{3} \rho k \quad \mu_{\text{eff}} \frac{\Delta U^{(m)}}{\Delta x^{(m)}} \tag{6}$$

$$\tau^{(ji)} \quad \mu_{lam}[g^{(jm)} \quad {}_{(m)}U^{(i)} \quad g^{(im)} \quad {}_{(m)}U^{(j)}] \tag{7}$$

The Reynolds turbulent stress tensor is derived by Boussinesq concept of turbulent viscosity:

$$\rho\overline{u^{(j)}u^{(i)}} \quad \mu_{\text{tur}}[g^{(jm)} \quad {}_{(m)}U^{(i)} \quad g^{(im)} \quad {}_{(m)}U^{(j)}] \tag{8}$$

The effective viscosity is derived from the following term:

$$\mu_{\text{eff}} = \mu_{\text{lam}} + \mu_{\text{tur}} \tag{9}$$

Turbulent viscosity is derived by the algebraic term:

$$\mu_{\text{tur}} \quad \frac{C_\mu \rho k^2}{\varepsilon} \tag{10}$$

where k and ε are turbulent kinetic energy and its dissipation rate, respectively, defined as:

$$k \quad \frac{1}{2} g_{(ij)} \overline{u^{(ij)} u^{(j)}} \tag{11}$$

and

$$\varepsilon \quad \nu_{\text{lam}} g_{(im)} g^{(jn)} \overline{{}_{(n)}u^{(m)} \quad {}_{(j)}u^{(i)}} \tag{12}$$

Presented mathematical model (tab. 1) has been solved numerically using BFC option of PHOENICS software.

Table 1. Governing equations with summarised standard and boundary layer *k*-ε turbulence model

Equation	Φ	Γ_Φ	S_Φ		
Continuity	1	0	0		
Momentum	$U^{(j)}$	μ_{eff}	$-g^{(ji)}\frac{\partial P}{\partial x^{(j)}}$ $[\rho U^{(j)}U^{(i)}$ $(\tau^{(ij)}$ $\rho\overline{u^{(j)}u^{(i)}})](\frac{i}{mj})$		
Turbulent kinetic energy	k	μ_{et}/σ_k	$G-\rho\varepsilon$		
Dissipation rate	ε	μ_{et}/σ_k	$\frac{\varepsilon}{k}(C_{\varepsilon 1}G$ $\rho C_{\varepsilon 2}\varepsilon)$		
G $g^{(ik)}$ τ^{ij}_{tur} $\frac{2}{3}g^{(ij)}(\rho k$ μ_{tur} $_{(m)}U^{(m)})$ $_{(j)}U^{(k)}$					
Model coefficients	σ_k	σ_ε	$C_{\varepsilon 1}$	$C_{\varepsilon 2}$	C_μ
– STKE	1.0	1.3	1.44	1.92	0.09
– BLKE	1.0	1.85	1.44	1.92	0.0324

Modifications of *k*-ε turbulence model applied to ABL

Atmospheric boundary layer (ABL) is defined [6] as "the region in which the atmosphere experiences surface affects trough vertical exchanges of momentum, heat and moisture". The traditional approach is to divide the ABL vertically into various layers, each characterized by different "scaling" parameters. The ABL can be divided into three major sublayers.

– The layer near ground up to the height of the roughness length. This layer has traditionally been referred to as a "laminar sublayer" or "roughness layer". Actually, in this layer molecular viscosity hardly plays a role and turbulent fluxes still occur, except very close to ground where the motion is primarily laminar. Within this layer, up to height z_0, turbulence is intermittent or not fully developed, therefore z_0 can be interpreted as the eddy size at the surface.
– The surface layer (SL) from z_0 to z_s, where z_s varies from about 10 m to 200 m. In this layer, the fluxes of momentum, heat, and moisture are assumed to be independent of height and the Coriolis effects is generally negligible.
– The transition (or Ekman) layer (TL) from z_s to z_i, where z_i varies from about 100 m to 2 km. In special situations, such as during thunderstorms, the boundary layer can extend into the stratosphere.

From the point of wind power assessment at micro (site area less than 10 km^2) and meso (area less 1000 km^2) sites, the surface layer is of primarily importance. The mean characteristic of surface layer is weak shear flow. By experimental results of Panofsky *et al*. [3, 7], the shear stress to kinetic energy ratio for is typically $-\overline{uw}/k$ 0.16–0.18, that implies value of C_μ = = 0.0256-0.0324 and consequently, the sets of the rest of model coefficients (tab. 1). The lower value is recommended to meso scale simulations, where the lower part of surface layer up to 10-50 m is bridged by standard log-wall functions [2], whereas the higher value is recommended to micro scale simulations where the grid resolutions near the surface is sufficiently high [4]. If we focus on micro scale simulations (Askervein case study), then $C_\mu = 0.0324$. The value of $C_{\varepsilon 2}$, determined from experiments with decaying grid turbulence, should be remained unchanged.

The diffusion coefficient σ_k (Prandtl number of turbulence kinetic energy), close to unity following Reynolds analogy, also should be remained unchanged. The rest of model coefficients can be deduced by knowing expression valid in the log-law region:

$$\kappa^2 \quad \sigma_\varepsilon \sqrt{C_\mu}(C_{\varepsilon 2} \quad C_{\varepsilon 1}) \tag{13}$$

where $\kappa = 0.4$ is the von Karman constant. Using above recommendations and also leaving $C_{\varepsilon 1}$ unchanged, the diffusion coefficient σ_ε (Prandtl number of dissipation rate) can be deduced from expression (13). New set of k-ε model coefficients is:

$$C_\mu = 0.0324, \sigma_k = 1.0, \sigma_\varepsilon = 1.85, C_{\varepsilon 1} = 1.44, C_{\varepsilon 2} = 1.92 \tag{14}$$

The k-ε turbulence model, defined in tab. 1 can be referred as "standard k-ε model of surface layer" (BLKE).

Besides standard k-ε model and it's atmospheric boundary layer modification, we will also use Chen-Kim modification of k-ε turbulence model and RNG k-ε turbulence model. Last two models will be summarized in tab. 2 and tab. 3 respectively.

Table 2. Summarized Chen-Kim turbulence model

Equation	Φ	Γ_Φ	S_Φ			
Turbulent kinnetic energy	k	μ_{et}/σ_k	$G - \rho\varepsilon$			
Dissipation rate	ε	μ_{et}/σ_k	$\rho\frac{\varepsilon}{k}(C_{\varepsilon 1}G \quad C_{\varepsilon 2}\varepsilon) \quad \rho C_{\varepsilon 3}\frac{G^2}{k}$			
$G \quad g^{(ik)} \ \tau^{ij}_{\text{tur}} \quad \frac{2}{3}g^{(ij)}(\rho k \quad \mu_{\text{tur}} \ {}_{(m)}U^{(m)}) \quad {}_{(j)}U^{(k)}$						
Model coefficients	σ_k	σ_ε	$C_{\varepsilon 1}$	$C_{\varepsilon 2}$	$C_{\varepsilon 3}$	C_μ
	0.75	1.15	1.15	1.9	0.25	0.09

Table 3. Summarized RNG turbulence model

Equation	Φ	Γ_Φ	S_Φ				
Turbulent kinetic energy	k	μ_{et}/σ_k	$G - \rho_\varepsilon$				
Dissipation rate	ε	μ_{et}/σ_k	$\rho\frac{\varepsilon}{k}(C_{\varepsilon 1}G \quad C_{\varepsilon 2}\varepsilon \quad \alpha\varepsilon)$				
$G \quad g^{(ik)} \ \tau^{ij}_{tur} \quad \frac{2}{3}g^{(ij)}(\rho k \quad \mu_{tur} \ {}_{(m)}U^{(m)}) \quad {}_{(j)}U^{(k)}$ $\alpha \quad C_\mu \eta^3 \frac{\frac{1}{\eta_0}\eta}{1 \quad \beta\eta^3}; \quad \eta \quad \frac{Sk}{\varepsilon}$ $S \quad \sqrt{\frac{1}{2}(\ {}_{(j)}U^{(i)} \quad {}_{(i)}U^{(j)})^2}$							
Model coefficients	σ_k	σ_ε	$C_{\varepsilon 1}$	$C_{\varepsilon 2}$	C_μ	η_0	β
	0.7194	0.7194	1.42	1.68	0.0845	4.38	0.012

Askervein case study

Site description

Askervein, or Askernish hill as it is sometimes referred to locally, is located near the west coast of South Uist, toward the southern end of the Outer Hebrides island chain of Scotland. The hill coordinates are 57°11'N, 7°22'W. It is essentially elliptical in plan form with 1 km minor axis and 2 km major axis. The major axis is oriented along a generally NW-SE line. The predominant wind directions during September and October (the period of the experiments) are from the SW and S. The digital elevation model, a portion of which is shown as fig. 1, shows that the hill is relatively isolated, apart from the hills to the NE and E, *i. e.*, downstream of the prevailing wind direction. The hill top (HT) is at a height of 126 m above sea level. Since HT is somewhat to the NW end of the hill, a second reference location ('centre point' or CP) was chosen as an additional point of reference on hill. During the experiments, most of the masts were deployed in approximately linear arrays through CP or HT. The mean lines chosen were oriented at 043° (grid) and 133° (grid), approximately NE-SW and SE-NW along the minor and major axes of hill, respectively. They are shown in fig. 1 and referred to as lines A, AA and B, as shown.

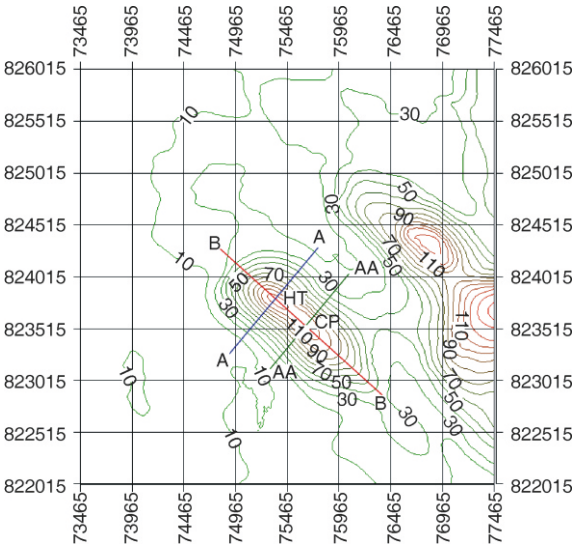

Figure 1. Lines of installed masts at Askervein hill

Askervein project

Askervein project was a collaborative study carried out under the auspices of the International Energy Agency Programme of R&D on Wind Energy Conversion System [5]. The experiments were conducted in 1982 and 1983. Askervein is the site of the most complete field experiment to date, with 50 masts deployed, and whose 27 of them were equipped with three component turbulence sensors. Askervein '83 was conducted between September 14 and October 18, with mean observational runs in the period September 25-October 10. All of the designated runs over the 16 day period provided good and interesting data covering a range of wind directions. Monday, 3 October was perhaps the "best" day for data collection with steady, moderate-to-strong winds (10 m/s) from 210° trough most of the day. Richardson number was varying from 0.0131 to –0.011. These results have been used in many verification and testing of different models, both numerical and experimental (wind tunnel experiments), therefore this case is particularly well documented. This made the Askervein hill case the most suitable reference to test numerical results *vs*. full scale experimental data when it comes to micro scale modelling. For this study, three sets of data have been available: (a) normalized velocity values at 10 meters

height along the A line; (b) normalized velocity values at 10 meters height along the AA line; and (c) fractional speed up at the hill top (HT).

Numerical setup and boundary conditions

The physical domain is discretised by 100*100 grid cells covering area of 2 2 km with the $x_1 - x_2$ plane. The height of domain is fixed at 1 km, with 30 uniform grid resolution of 20 m in 21 grid cells with variable geometrical distribution. In this study, the recommendation of grid resolution tests [3] has been accepted having minimum 3 cells in the first 10 m above ground surface.

Equilibrium wall-functions have been used as the boundary conditions at the ground surface.

Upper and outlet boundary conditions are specified by von Neumann conditions (zero first derivatives of all variables). Lateral inlet profiles of velocity, turbulence kinetic energy and its dissipation rate are specified by the following analytical expressions [1]:

$$U_1(x_3) \quad \frac{u_\tau}{\kappa} \ln \frac{x_3}{z_0} \quad \text{for } x_3 \quad 500\ \text{m}$$
$$U_1(x_3) \quad 10\ \text{m/s} \quad \text{for } x_3 \quad 500\ \text{m} \tag{17}$$

$$k(x_3) \quad \frac{u_\tau^2}{C_\mu} \; 1 \quad \frac{x_3}{H}^2 \tag{18}$$

$$\varepsilon(x_3) \quad \frac{u_\tau^3}{\kappa} \; \frac{1}{x_3} \quad \frac{4}{L_{MO}} \tag{19}$$

where friction velocity u_τ = 0.4423 m/s is deduced by (17), H is domain height and is L_{MO} Monin-Obukov length scale taking equal to H.

Presentation of results

Normalized velocity along the A and AA lines as well as fractional speed up parameter at HT are shown on figs. 2-4, respectively. Velocity along the A- and AA-lines are normalized by reference velocity.

The fractional speed-up parameter is calculated by expression:

$$\Delta S(h) = [V(h) - V_{ref}(h)]/V_{ref}(h) \tag{20}$$

Generally speaking, based on the shown diagrams, it can be concluded that no significant gain is obtained by CKKE and RNG model, comparable to STKE, whereas the BLKE shows the most promises that should be ex-

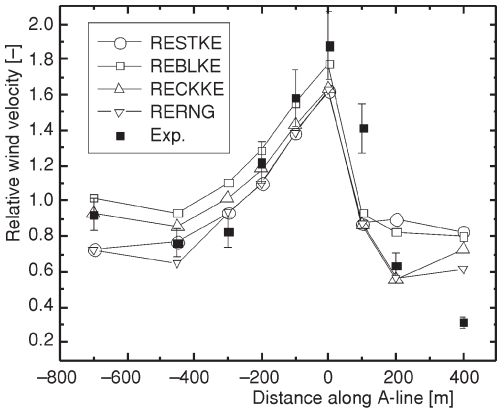

Figure 2. Normalized velocity along A-line with different turbulence models

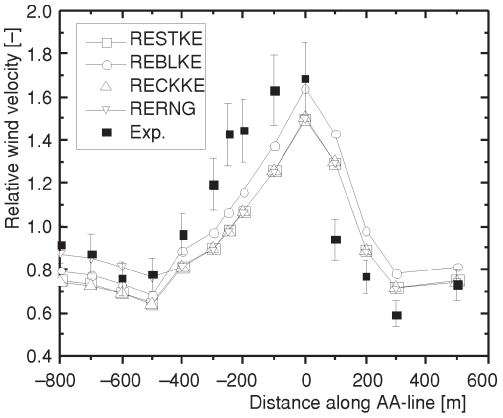

Figure 3. Normalized velocity along AA-line with different turbulence models

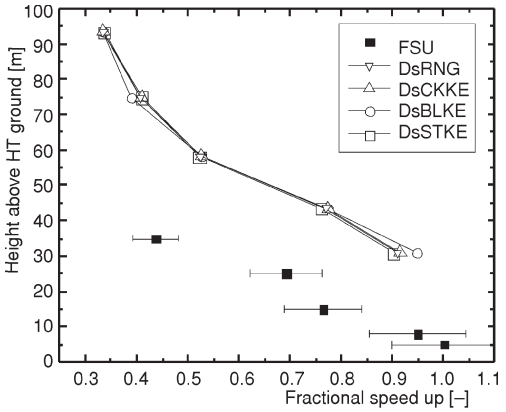

Figure 4. Fractional speed-up above top hill

pected due to model coefficient set up for weak shear flow of atmospheric boundary layer. The relative velocity at both lee-ward and wind-ward sides along A-line is acceptable, whereas at the HT is under-predicted. However, relative velocity is under predicted at wind-ward side and over predicted at lee-ward side along AA-line, but at the CP, it is quite correct. Fractional speed-up parameter at HT is, generally, under predicted with tendency to be closed to experimental data at the higher height.

Conclusions

The present paper is intended to provide a comparison of basic results of the Askervain hill project and the results of numerical simulation in which standard k-ε turbulence model, as well as three modifications of that model, were used to simulate the flow. Among these numerical results the best predictions were those of BLKE model, which was not surprising, but inspite of that fact an increasing of accuracy is needed, which may be obtained by better tuning of model coefficients.

It is also stressed in this paper that the velocity field on Askervein may be affected by the neighboring hills downwind. These hills may probably produce some upwind blockage (fig. 1). Actually, in most cases, the speed on the hill top is under-predicted. This could be related with the fact that the topography around the site is not correctly taken into account with smaller micro-model.

As in [3], it is pointed out that a lower roughness gives better results for the hill top in a study on the Askervein hill case; there are still questions about the roughness length that should be adopted. A lower roughness seems to give better results for the hill top.

Further improvements may be accomplished by introducing considerations of unstable atmospheric conditions, where temperature becomes active scalar, producing additional buoyancy driven flow. It implies that there is an additional time scale of bouncy effects. The fluctuating body force permits the work that must be added as a source term in the budget of turbulence kinetic energy.

Note that as long as wind energy assessment is the matter of interest, the most important point is to predict maximum speed up in the right locations, if possible, with good accuracy.

The details of flows on the lee-ward side is not relevant for such an application. However, in the interest of micro scale modelling aimed at other purposes-such as pollutant dispersion, the study of other cases may be desirable.

Acknowledgment

This paper is concerned by the National Program of Energy Efficiency, project number: NPEE-273013.

References

[1] Launder, B. E., On the Effects of a Gravitational Field on the Turbulent Transport of a Heat and Momentum, *Journal of Fluid Mechanics, 3* (1975), pp. 569-581
[2] Detering, H. W., Etling, D., Atmospheric Boundary Layer, *Boundary Layer Meteorology, 33* (1985), pp. 113-133
[3] Lumley, J. L., Panofsky, H. A., The Structure of Atmospheric Turbulence, Interscience Monographs and Text in Physics and Astronomy (Ed. R. E., Marshak), Vol. XII, John Wiley & Sons Inc., New York, USA, 1964
[4] Leroy, J. Gravdahal, A. R., Wind Field Simulations at Askervein Hill, Technical Report: VECTOR_9910_100, VECTOR AS, Tonsberg, Norway, 1999
[5] Taylor, P. A., Teunissen, H. W., The Askervein Hill Project: Overview and Background Data, *Boundary Layer Meteorology, 39* (1987), pp. 15-39
[6] Zannetti, P., Air Pollution Modeling: Theories, Computational Methods and Available Software, Van Nostrand Reinhold, 1990
[7] Panofsky, H. A., Tennekes, H., The Characteristics of Turbulent Velocity Components in the Surface Layer under Convective Conditions, *Boundary Layer Meteorology, 11* (1977), pp. 355-361

Paper submitted: January 19, 2009
Paper revised: January 22, 2009
Paper accepted: May 02, 2009